ATLAS Internal Note
LARG-No-084
13th October, 1997

A study of the presampler intersector crack

A. Ferrari
ISN Grenoble, France

J. Söderqvist
KTH Stockholm, Sweden

Abstract

The influence of the crack between the ATLAS barrel liquid argon presampler sectors is studied. A calculation of the electric field is performed, which allows a realistic estimation of the charge collection between the lateral edges of the electrodes and the inner surface of the skirt which separates one presampler sector from another. A GEANT simulation of electrons in the intersector gap shows that the effect of the crack on the energy measurement in the presampler is small.

1 Introduction.

The presampler detector is a 11 mm thin active layer of liquid argon in front of the accordion calorimeter and corrects for the energy lost in the material in front of the calorimeter. In the transverse plane, it has a polygonal shape formed by 32 identical azimuthal sectors per half-barrel, each sector spanning 0.2 in ϕ and 1.51 in η. A sector is made of 8 modules : each of the modules 1 to 7 covers 0.2 in η, while the module 8 at the outer end of the barrel covers 0.11 only. The charge deposited by electromagnetic showers in the 11 mm thin active layer is collected by 277.5 mm long electrodes which are arranged transversally with respect to the longitudinal axis. The gap between these electrodes is kept approximately identical at a value of 2 mm throughout the device, allowing to operate the presampler with a fixed high-voltage of 2 kV. The electrodes are perpendicular to the longitudinal axis, except for the modules covering $-0.4 < \eta < 0.4$ where they are slanted. Each of the supermodules has a kevlar skirt which protects the electrodes. This skirt covers the inner surface of the presampler and the edges where the modules meet. More details about the presampler construction can be found in the Liquid Argon Calorimeter TDR [1].

As shown on figure 1, there is a gap between the presampler sectors in the ϕ-direction. At the temperature of liquid argon, this gap is about 1.8 mm wide : the clearance between the skirts of the sectors is around 1 mm, while the skirt thickness is 0.4 mm. In this region, no charge can be collected and, consequently, all the energy deposited there by electromagnetic showers is lost. Furthermore, the distance between the skirt inner surface and the copper edge of the anode is 2 mm. By making the inner surface of the skirt conductive and connecting it to the ground compared to the 2 kV potential of the anode, charge collection in this region is possible, which reduces the effect of the intersector gap.

In this note, the electric field and the charge collection are determined in the intersector region. To study the effect of the crack on the energy measurement of electrons in the presampler, a GEANT [2] simulation using the DICE 95 [3] framework has been performed.

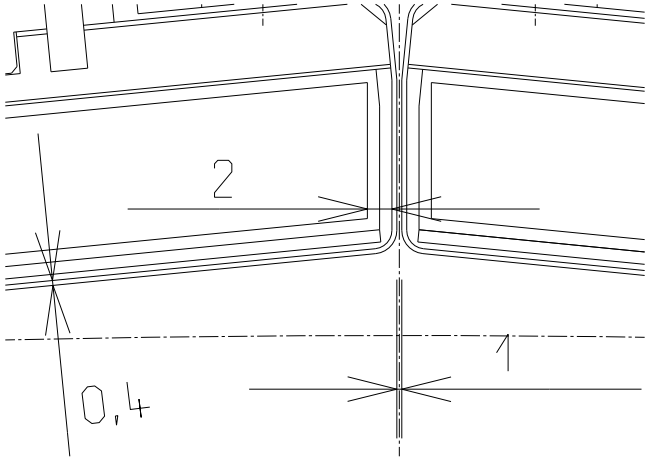

Figure 1: Zoom of the crack between the presampler sectors.

2 Charge collection in the presampler cracks.

In order to estimate the charge collection, a two-dimensional map of the electric field is calculated using the PRIAM package [4], which solves two-dimensional Poisson equations using a finite elements method. The collected signal depends on the charge drift and the filtering performed by shapers in the electronic readout chain. Considering these effects, an effective charge collection can be estimated.

2.1 Signal induced by charges drifting in an electric field.

The presampler anodes and cathodes (or the grounded skirt) can be sketched as shown in figure 2. A charge q_0, which is at position $\vec{r}$ at time t and which is drifting with a velocity $\vec{v}$ in a local electric field $\vec{E}$, induces an instantaneous current $i(t)$ given by [5] :

$$i(t) = \frac{q_0}{V_0}\vec{E} \cdot \vec{v}(\vec{E}) \tag{1}$$

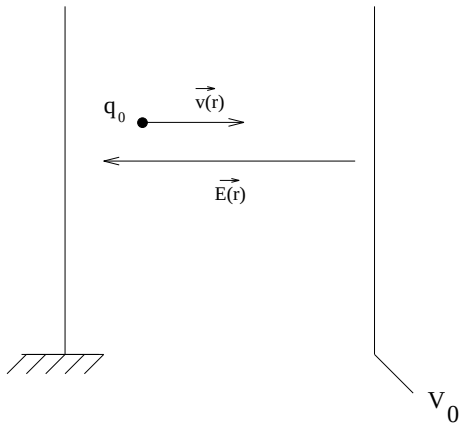

Figure 2: Sketch of a charge drifting between the presampler anodes and either cathodes or grounded skirt.

In the following, $\vec{E}$ and $\vec{v}$ are assumed to be parallel. The NA48 collaboration has measured [6] :

$$v\ [\mathrm{mm}/\mu\mathrm{s}] = 0.1809 \times E \times \ln(1 + \frac{8.975}{E}) + 1.4614 \times E^{0.329} \text{ with E in kV/cm} \tag{2}$$

If the electric field $\vec{E}$ is uniform, $i(t)$ remains constant until q_0 reaches the anode. As a result, if one assumes that the ionisation is uniform all along a track, all the charges produced give a triangular shaped current $I(t)$. The signals are then filtered with an integrating preamplifier followed by a bipolar shaper. For the presampler, the shaping function s can be expressed as [7] :

$$s(x) = \left(\frac{x^2}{2} + \frac{x}{\lambda - 1} + \frac{\lambda}{(\lambda - 1)^2}\right)\frac{e^{-x}}{\lambda - 1} - \frac{\lambda e^{-x/\lambda}}{(\lambda - 1)^3} \tag{3}$$

Here $x = t/\tau$ and $\lambda = \tau_{pa}/\tau$: τ is the shaping time and $\tau_{pa} = R_0 C_d$, where R_0 is the cable characteristic impedance and C_d is the detector capacitance.

The output signal[1], which is related to the total collected charge and thus the deposited energy, can be defined by :

$$\text{Signal} \equiv I_{eff}(t_P) = \int_0^{t_P} I(t')s(t_P - t')dt' \tag{4}$$

where t_P is the peaking time of $I_{eff}(t)$, from 0 to 100%.

In the case of a homogeneous electric field, the shapes of $I(t)$ and $I_{eff}(t)$ are shown on figure 3. Here, the calculation is done for module 5, which covers $0.8 < \eta < 1.0$ and for which $\tau_{pa} = 11.1$ ns, $\tau = 13$ ns and $t_P = 36.4$ ns [8].

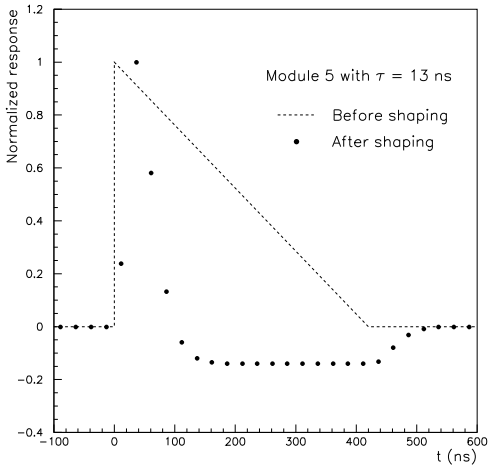

Figure 3: Normalised current response of the presampler, before and after shaping : the showers are supposed to be located in a region where the electric field is homogeneous. For the response after shaping, each dot corresponds to a bunch-crossing.

If a charge drifts in a non-homogeneous electric field, the current $i(t)$ is not constant anymore. When a charge q_0, created in the crack, drifts towards the anode, the electric field increases and so does $i(t)$. To derive the signal, a numerical integration in two steps is necessary. First, for each charge q_0 created in the non-homogeneous electric field, the individual signal $i_{eff}(t_P)$ must be calculated following the charge along its drift line until t reaches t_P. The total signal $I_{eff}(t_P)$ is then obtained by adding the contributions of all the charges created in the shower:

$$I_{eff}(t_P) = \sum_{\text{charges}} i_{eff}(t_P) = \sum_{\text{charges}} \int_0^{t_P} i(t')s(t_P - t')dt' \tag{5}$$

A uniform ionisation is assumed in the crack.

[1]The equivalent current is used for the shaper output, which is an amplified voltage in reality.

2.2 The signal map in the presampler crack.

The crack region treated in this note has a non-homogeneous electric field. As stated earlier, two dimensional fields can be calculated with the PRIAM package. The crack region therefore needs to be simplified : to the first order, the field perpendicular to the longitudinal axis can be assumed to be constant. The resulting two-dimensional geometry of the crack region and the electric field map in the (η, ϕ) plane are shown in figure 4.

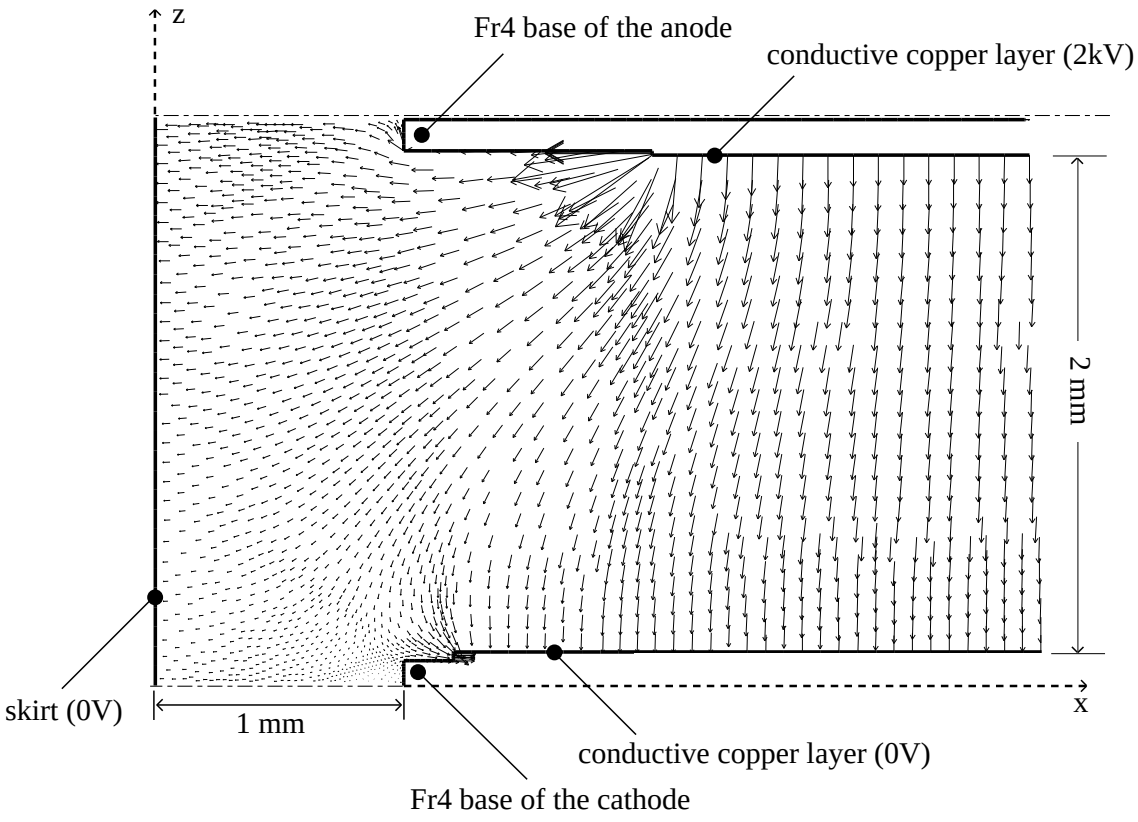

Figure 4: Electric field map in the presampler crack region : the x-axis corresponds to the ϕ-direction, while the z-axis corresponds to the η-direction : the arrows are vectors showing the direction and the strength of the local electric field.

Using the method described in section 2.1, the resulting signal $i_{eff}(t_P)$ can be estimated for charges located in each point of the crack region, as shown in figure 5.

To simplify, assume that the ionisation is uniform along the η-direction for each readout cell of the presampler in the crack, so that an average signal response in the ϕ-direction is derived by adding the contribution of all the points along the η-direction. The mean signal response along ϕ is shown in figure 6, where the signal have been normalized to 1 in the zone in between the anode and the cathode where the electric field is homogeneous.

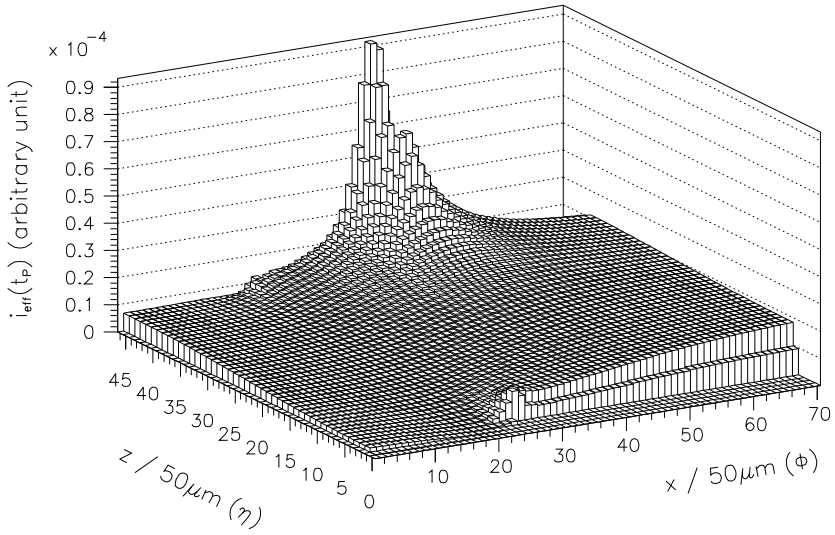

Figure 5: Signal map in the presampler crack region, derived from the values of the electric field in the crack region, after charge collection and signal filtering. The x and z-directions are the same as in figure 4.

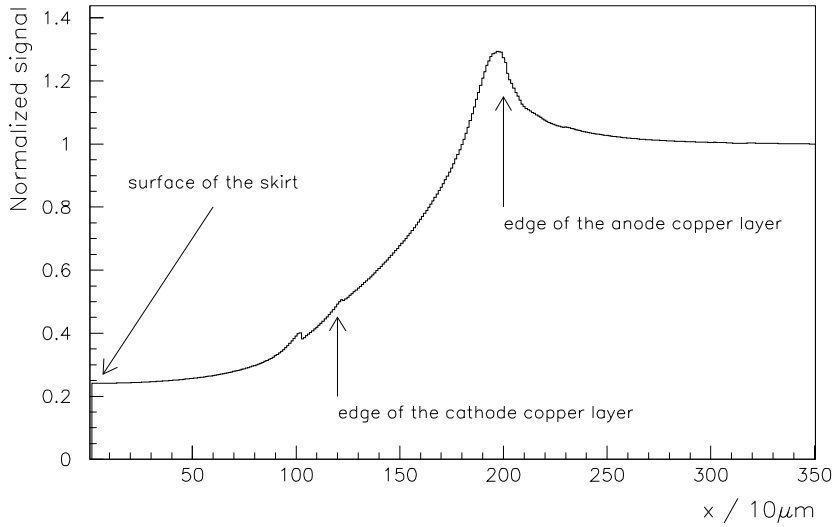

Figure 6: Variation of the signal along the ϕ-direction (x-axis) in the crack, assuming uniform ionisation along η.

3 Energy loss in the presampler crack region.

To derive the fraction of energy lost in the crack, a GEANT simulation of the ATLAS detector is performed using the DICE 95 framework (version 96_12 is used for the detector geometry). The standard presampler geometry is changed so that sensitive liquid argon volumes are introduced in the crack. Thus, all the energy deposited in the crack can be measured and a comparison can be done between the ATLAS designed presampler and an "ideal" detector without any crack. Following the notation of the previous section for the ϕ-direction (x-axis in figures 4-6), the fully dead region (gap between protection skirts and skirts) covers $-0.9 < x < 0$ mm and the region with reduced charge collection covers $0 < x < 3.1$ mm. Two mirror imaged configurations like this give a 8 mm wide crack region. Thus, half of the crack is a 4 mm wide volume, which in the simulation is divided into 40 sensitive divisions, each of them having a 100 μm width in the ϕ-direction. Figure 7 shows a transverse cut of the presampler geometry, as described in DICE 95.

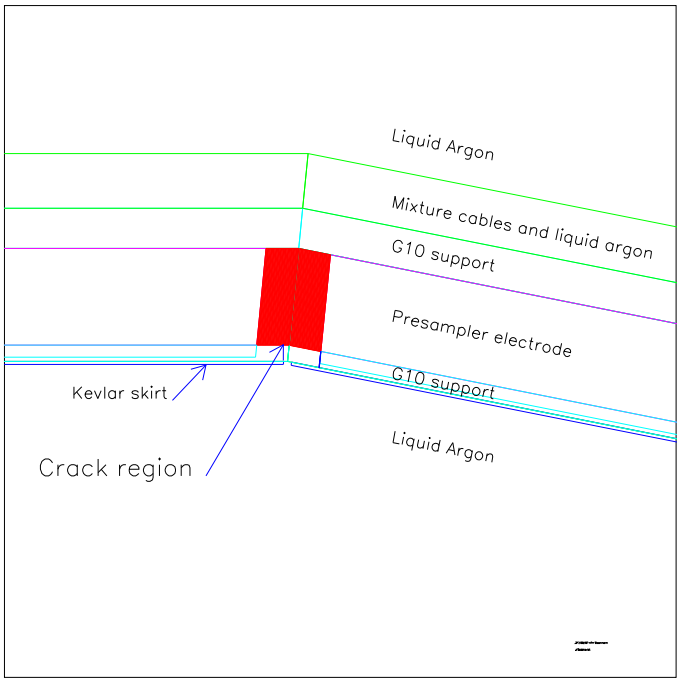

Figure 7: Presampler crack geometry as described in DICE 95.

To account for the charge collection calculated in the previous section, a signal response weight w_j is given to each of the sensitive divisions in the crack. The weight w_j is the mean value of the signal response in the slice. The fraction of energy which is not measured because of the crack is then given by :

$$\rho = \frac{E_{lost}}{E_{presampler}} = \frac{\sum_{j=1}^{40}(1-w_j)E_{crack}(j)}{E_{PS} + \sum_{j=1}^{40}E_{crack}(j)} \tag{6}$$

Electrons of various energies have been generated at $\eta = 0.9$, in the crack region. To allow a precise determination of the electron shower position in the crack, the magnetic field has been switched off. This makes the simulation somewhat less realistic. However, the magnetic field usually spreads secondary charged particles over a larger region. Thus, the maximal loss determined here should be a conservative estimate.

Figure 8 shows which fraction of the energy is measured by the presampler, for three different transverse energies $E_T = 5$, 10 and 20 GeV and when the generated angle is between 0.088 and 0.108 (the middle of the intersector gap corresponds to $\phi = 0.098$). A cut of 10 MeV is applied on the total energy deposited in the presampler (this cut corresponds to approximately 4 m.i.p's). Notice that the loss in the crack increases when E_T increases. The greater the energy is, the later the shower starts to develop in the cryostat and the narrower the shower is. Therefore, the maximal loss is slightly larger.

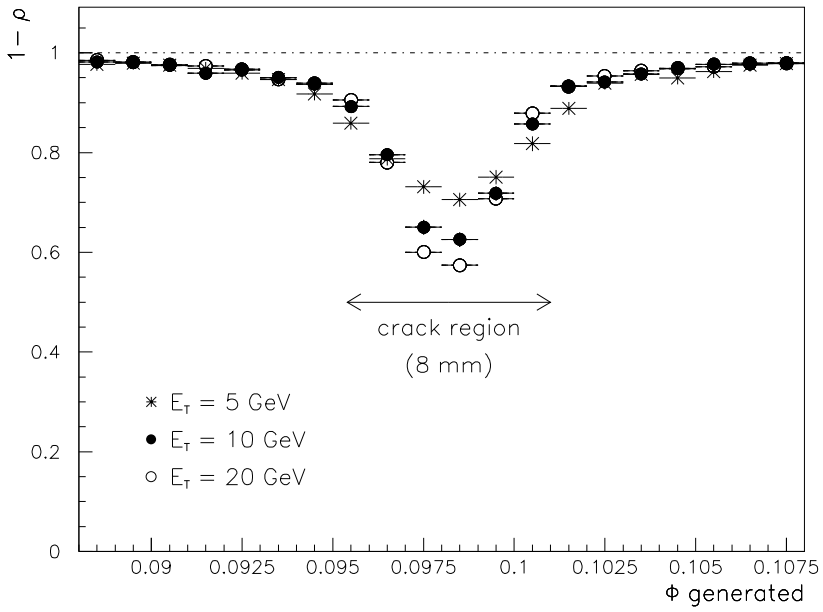

Figure 8: Average energy collected in the presampler as a function of the position of the electromagnetic shower in the crack. Electrons with transverse energy $E_T = 5$, 10 and 20 GeV have been generated at $\eta = 0.9$. A cut of 10 MeV is applied on the total energy deposited in the presampler.

The total surface of the cracks is about 1.5% of the total surface of the barrel presampler. To study the impact of the cracks on the energy measurement in the whole presampler, 10000 electrons with $E_T = 10$ GeV have been generated at $\eta = 0.9$ and the full 2π in ϕ, with the magnetic field switched on. Figure 9 shows the probabilities of mismeasuring the presampler energy because of the cracks.

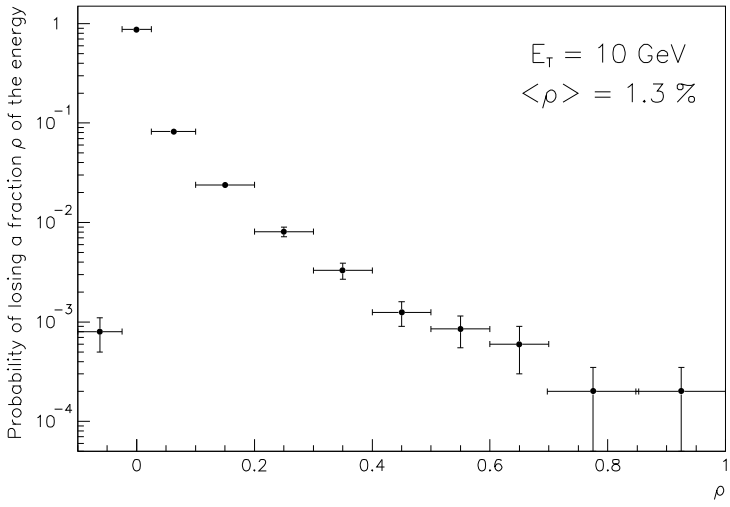

Figure 9: Probability that a fraction ρ of the presampler energy is lost due to the cracks. Electrons with $E_T = 10$ GeV have been generated at $\eta = 0.9$ and a cut of 10 MeV is applied on the total energy deposited in the presampler. If electrons create charges near the edge of the anode, where the charge collection is maximal, energy can be gained and ρ can be negative.

4 Comparison with the official presampler geometry in DICE 95.

In the official DICE 95 geometry (versions 96_3 to 97_6), the crack is a 3 mm wide region, which is completely dead. The kevlar skirts are included in the crack description and all the liquid argon in this region is dead.

The effect of the 8 mm crack with a realistic charge collection is compared to the effect of a 3 mm completely dead crack in figure 10, for electrons generated at $\eta = 0.9$ with $E_T = 10$ GeV and with the magnetic field switched off. The 3 mm completely dead crack gives slightly smaller losses than the 8 mm crack with charge collection, but the difference is small. Furthermore, the shapes of the energy loss along the ϕ-direction are very similar for the two geometries.

The average loss obtained in the case of the 3 mm dead crack is 1.1% as shown in figure 11, compared to 1.3% for the crack described in section 3. The average loss $< \rho >$ depends on the width of the dead crack, as shown in figure 12. If the width of the dead crack was 3.6 mm, the energy loss would closely resemble the energy loss from the real 8 mm crack, with charge collection between the anodes and the kevlar skirt. Figure 13 shows the presampler geometry with a 3.6 mm dead crack. This tuned width of the crack will be included in future releases of the DICE 95 presampler geometry.

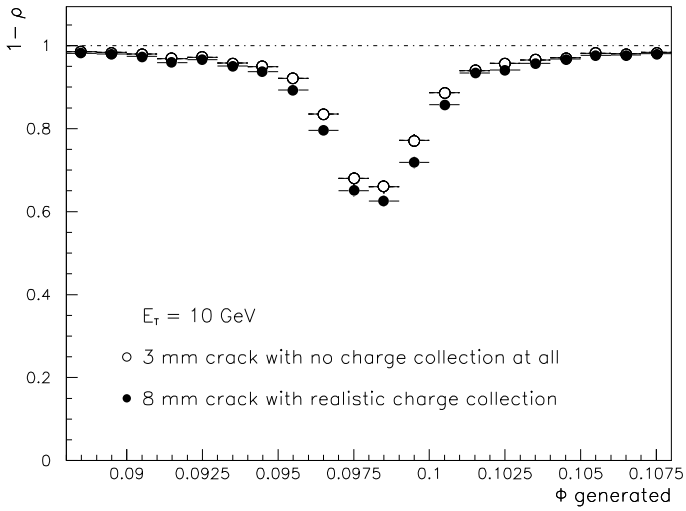

Figure 10: Fraction of the average energy collected in the presampler as a function of the electron impact in the crack for a 8 mm wide region with charge collection (filled circles) and a 3 mm wide completely dead crack (open circles). The response is given for electrons having a transverse energy of 10 GeV and generated at η=0.9. A cut of 10 MeV is applied on the total energy deposited in the presampler.

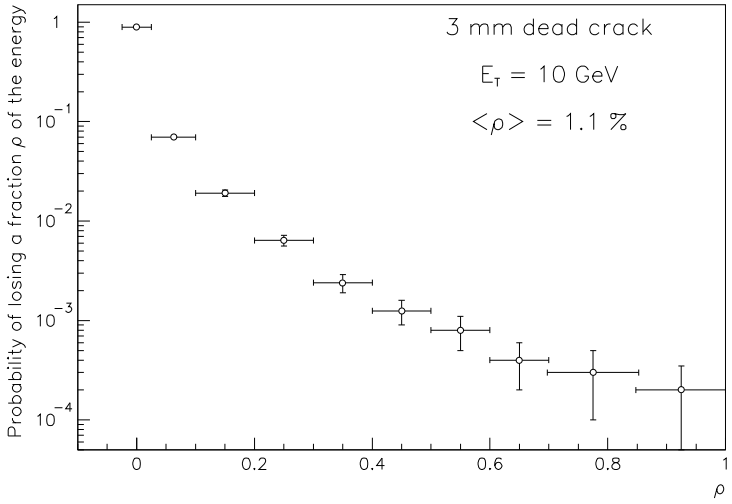

Figure 11: Probability that a fraction ρ of the presampler energy is lost in a 3 mm completely dead crack. The transverse energy of the electron and the cuts are the same as in figure 9.

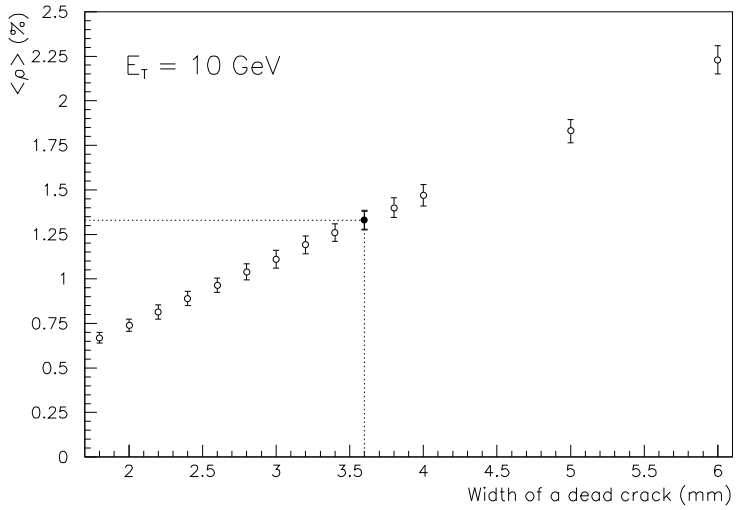

Figure 12: Average probablity for loosing a certain fraction of the energy in the presampler as a function of the "tuned" width of a completely dead crack. If the width is tuned to 3.6 mm, then the average loss is similar to the one obtained using a realistic 8 mm crack.

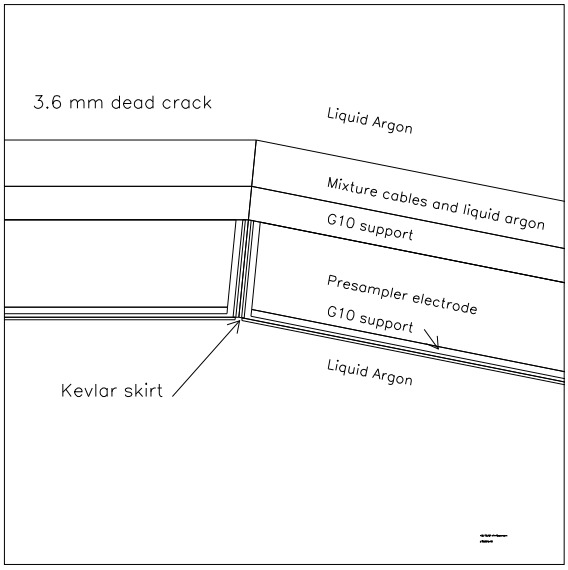

Figure 13: Transverse cut of the presampler when the crack is a 3.6 mm wide completely dead region, with the kevlar skirts inbetween the presampler sectors.

5 Comments on the combined presampler and EM-calorimeter measurement.

The energy of interest for physics is the one measured by the complete calorimeter system, where the measurements of the presampler and the accordion calorimeter are combined. The presampler is only used to correct for the energy lost before the calorimeter. Only if the energy lost is large (which means that the electron showered before the calorimeter), the presampler measurement is important. But, if the electron showers, the fraction of energy which is likely to be lost in the crack region is small, since the shower is generally smeared over an area larger than the crack. This is shown in [9,10], where the lost energy considered is a fraction of the total energy deposited in the calorimeter system. In that simulation, a completely dead region of 2 mm was considered. This optimistic crack width gives approximately 25% too small losses for the presampler but one can still safely conclude that the presampler crack has a small effect on the overall calorimeter performance. In this note, the effect of the presampler crack region has been treated in a more realistic way, considering a larger crack which closely resembles the final presampler design but taking the charge collection in the crack into account. The main result is that the influence of the cracks on the energy measurement in the presampler is small.

6 Conclusion.

The effect of the crack between presampler sectors has been studied in detail for the presampler engineering design. The local electric field has been calculated and the resulting charge collection in the crack has been determined. Taking the varying charge collection into account, a GEANT simulation shows that the effect of the crack on the presampler energy measurement is very small. We conclude that a sophisticated treatment of this crack will not be necessary in future simulations of the ATLAS detector. The width of the dead crack in the GEANT simulation has been tuned to 3.6 mm in order to give the same effect as the engineering designed presampler.

Acknowledgements.

We would like to thank Guy Lemeur (LAL, Orsay) for his help with the field calculations. We also acknowledge Bengt Lund-Jensen (KTH, Stockholm) and Johann Collot (ISN, Grenoble) for their advices and the fruitfull discussions we had concerning this work.

References.

[1] ATLAS Liquid Argon Calorimeter Technical Design Report, CERN/LHCC/96-41, 15 December 1996.

[2] R. Brun et al., GEANT3, CERN DD/EE/84-1 (1986).

[3] A. Artamonov, A. Dell'Acqua, D. Froidevaux, M. Nessi, P. Nevski and G. Poulard, "DICE-95 : A modified DICE framework", ATLAS-SOFT/95-14, 15 January 1996.

[4] G. Lemeur, F. Touze : Status and perspectives of the PRIAM/ANTIGONE codes, Computational Accelerator physics, Williamsburg, Virginia, 1996 (J.J. Bisognano, A. Mondelli Ed.) AIP conference proceedings 391, p. 113-118.

[5] W.J. Willis and V. Radeka, NIM 120 (1974) 221-236.

[6] A.M. Kallin, Y.K. Potrebennikov, A. Gonidec and D. Schinzel, "Temperature and electric field strength dependence of electron drift velocity in liquid krypton and liquid argon", NA48 draft note.

[7] R.L Chase, C. de La Taille, J.P Richer, N. Seguin-Moreau, "A fast monolithic shaper for the ATLAS E.M calorimeter", ATLAS Internal Note LARG-NO-10.

[8] J. Collot (ISN Grenoble), private communication.

[9] Fig 2-14 p 38, ATLAS Calorimeter Performance, CERN/LHCC/96-40, ATLAS TDR 1.

[10] L.O Eek, B. Lund-Jensen, J. Söderqvist and A. Vaniachine, Optimisation of the presampler intersector gap geometry, LAr note in preparation.